NOTES AND CORRESPONDENCE

Diurnal Cycle of Oceanic Precipitation from SSM/I Data

A. T. C. CHANG

Hydrological Sciences Branch, Laboratory for Hydrospheric Processes, NASA/Goddard Space Flight Center, Greenbelt, Maryland

L. S. CHIU AND G. YANG

SAIC/General Science Corporation, Laurel, Maryland

9 September 1994 and 5 May 1995

ABSTRACT

Four and a half years of the global monthly oceanic rain rates derived from the DMSP (Defense Meteorological Satellite Program) *F-8* SSM/I (Special Sensor Microwave/Imager) data are used to study the diurnal cycles. Annual mean rainfall maps based on the SSM/I morning and evening observations are presented, and their differences are examined using a paired *t* test. The morning estimates are larger than the afternoon estimates by about 20% over the oceanic region between 50°S and 50°N, with significant differences located mainly along the intertropical convergence zone region. Using the measurements from two satellites, either DMSP *F-8* and *F-10* or DMSP *F-10* and *F-11*, amplitudes and phases of the 24-h harmonic are estimated. The diurnal cycle shows a nocturnal or early morning maximum in 35%–40% of the oceanic regions. Monte Carlo simulations show that the rms errors associated with the estimated amplitude and phase are about 100% and 2 h, respectively, mainly due to the large random errors (50%) associated with the present rainfall estimates and the nonoptimal separation times of the DMSP satellite sampling.

1. Introduction

The diurnal cycle of oceanic rainfall and its variation in different regions remains an important unanswered question regarding global precipitation. Because of the scarcity of rainfall data over the oceans, different parameters have been used as rainfall proxies to study the diurnal cycle. For example, Riehl and Miller (1978), Albright et al. (1985), Meisner and Arkin (1987), Shin et al. (1991), and Janowiak and Arkin (1991) used satellite infrared data; Short and Wallace (1980), Hartmann and Recker (1986), and Gruber and Chen (1988) relied on outgoing longwave radiation data; Gray and Jacobson (1977) used rain gauge data; McGarry and Reed (1978) examined radar data collected during GATE [GARP (Global Atmospheric Research Program) Atlantic Tropical Experiment]; Kraus (1963) analyzed weather ship data; and Kidder and Vonder Haar (1977) and Sharma et al. (1991) used passive microwave data.

It is generally believed that the diurnal cycle in oceanic deep cumulus convection is small because the oceanic lower-tropospheric lapse rate does not undergo significant diurnal variation. Kraus (1963) analyzed rainfall records of nine weather ships and found that maritime precipitation is significantly more frequent at night. He argued that the nocturnal maximum is due to destabilization of the tropospheric lapse rate by longwave cooling that dominates the radiative balance after solar heating is cut off. Although the available weather ship records came from northern temperate latitudes, Kraus believed there is no evidence for a different daily pattern over the open tropical and southern oceans.

Gray and Jacobson (1977) found strong early morning maxima in deep convection in the Tropics from gauge data collected at small, isolated tropical islands. The more intense the convection and the stronger the association with organized weather systems, the more intense is the diurnal cycle. In many places, heavy rainfall was two to three times greater in the morning than in the late afternoon to evening.

Albright et al. (1985) used the fractional cold cloud coverage determined from the GOES-West geostationary satellite to demonstrate a pronounced diurnal cycle over the central tropical Pacific. In the intertropical convergence zone (ITCZ) the cycle was found to have a distinct morning maximum and evening minimum. In other areas, such as the South Pacific convergence zone (SPCZ), an afternoon maximum was observed. Jan-

Corresponding author address: Dr. Alfred T. C. Chang, Hydrological Sciences Branch, Laboratory for Hydrospheric Processes, Code 974, NASA/GSFC, Greenbelt, MD 20771.

owiak and Arkin (1991), using infrared data from the GOES (Geostationary Operational Environment Satellite), GMS (Geostationary Meteorological Satellite), and Meteosat geostationary satellites, reported the preferred time for more intense convection is earlier in the day.

Shin et al. (1991) computed the diurnal cycle from three hourly histograms of GOES data. Over most of the central Pacific, the 24-h harmonic dominates. In regions where the 24-h harmonic is statistically significant, the phase associated with this harmonic peaks in the early to late afternoon. Coincidentally, the 12-h harmonics are also important, with peaks centered around 0600 and 1800 LT. This suggests that monthly area-averaged rainfall estimates from sun-synchronous low-orbiting satellites will include a bias due to the existence of the semidiurnal cycle. In the SPCZ and ITCZ the bias due to the semidiurnal cycle is about 5%–10%.

Sharma et al. (1991) examined the diurnal cycle using one year (July 1987–June 1988) of the Defense Meteorological Satellite Program (DMSP) Special Sensor Microwave/Imager (SSM/I)–derived rainfall data. By averaging over a large area to reduce the random errors in the estimates, the average ratio of morning to afternoon rainfall was about 1.2. This is not nearly as large as the factor of 2–3 reported by Gray and Jacobson (1977) in some areas. Microwave emissions from the ocean surface at 53° incidence angle are highly polarized. However, emission from raindrops are usually not polarized. Petty and Katsaros (1992) used the 37-GHz polarization differences of the SSM/I data to extract rainfall information. Pixels that exhibited a 37-GHz polarization difference (vertically polarized brightness temperature minus horizontally polarized brightness temperature) of less than 15 K were assumed to indicate moderate to intense precipitation over the oceans. For the period of 20 July–19 August 1987 Petty and Katsaros (1992) found the ratio of the number of precipitation pixels for morning and afternoon was about 1.27 over oceans between ±60° latitude.

Mapes and Houze (1993) examined very cold (<208 K) and moderately cold (<235 K) cloud clusters in the oceanic warm pool region between 80°E and 160°W from IR imagery. They found that the diurnal cycle of large (size greater than 20 000 km^2) very cold clouds is a sun-synchronous process. Deep convection of these very cold clouds peaks at dawn and decreases throughout the morning. The diurnal cycle of the moderately cold cloud clusters is dominated by the contribution from the largest clusters (size greater than 65 000 km^2), which peaks in the afternoon. The small moderately cold clouds shows very little diurnal variability.

Recently, Hendon and Woodberry (1993) reported results of an analysis of the diurnal cycle of tropical convection using an index of deep convective activity and a global cloud index. They concluded that over the tropical oceans the diurnal cycle is weak. Nonetheless, oceanic convection exhibits a systematic diurnal fluctuation with maximum intensity in the early morning.

In summary, previous investigators have shown that diurnal rain variations over the oceans are important. The diurnal amplitude may reach or exceed half of the mean value. Most of the results show nocturnal or early morning maxima, except those of Shin et al. (1991), which are based on IR histograms and the moderately cold super cloud clusters reported in Mapes and Houze's (1993) study. Infrared and visible sensors observe the cloud-top parameters, which are routinely affected by cirrus anvils and blowoff of convective towers. Microwave techniques, which are known to offer a more direct relationship with hydrometeors, are deemed to provide better rainfall estimates. However, microwave sensors onboard satellites with sun-synchronous orbits could at most sample the rainfall twice daily. Aliasing from diurnal variations such as the semidiurnal variation due to the sampling could limit the accuracy of time average rainfall estimates.

Recently, 4.5 years (July 1987–December 1991) of rainfall estimates from DMSP *F-8* SSM/I data have become available (Wilheit et al. 1991; Chiu et al. 1993). In addition, during 1991 and 1992, two SSM/I instruments were flown simultaneously. In 1991, the DMSP SSM/I *F-8* and *F-10* were in orbit. In 1992, both the DMSP SSM/I *F-10* and *F-11* were in orbit. When SSM/I observations from two satellites are available, four rainfall estimates per day with different observation times can be fitted to a simple diurnal cycle model consisting of only the mean and 24-h harmonic. SSM/I rainfall estimates for two separate months are harmonically analyzed to determine the phase and amplitude of diurnal variations. The errors associated with the amplitude and phase estimates are examined using Monte Carlo calculations.

2. Data

The DMSP *F-8* satellite was launched into near-circular orbit in June 1987 with passes overflown each earth location twice per day, around 0600 and 1800 (LT). The DMSP *F-10* satellite was launched into a slightly elliptical orbit in November 1990. Its equator crossing time drifted slowly from about 0755 LT in May 1991 to about 0830 LT in May 1992. The DMSP *F-11* satellite, with orbital characteristics similar to that of *F-8*, was launched into orbit in December 1991. Rain-rate estimates from SSM/I data were derived from the morning and evening passes separately. Four and a half years of rain-rate estimates based solely on the *F-8* SSM/I data (July 1987–December 1991, except in December 1987 when the SSM/I was turned off due to instrument temperature problem) were used for this study. Data from the *F-8* and *F-10* satellites and *F-10* and *F-11* satellites were used to extract the harmonic components of May 1991 and May 1992, re-

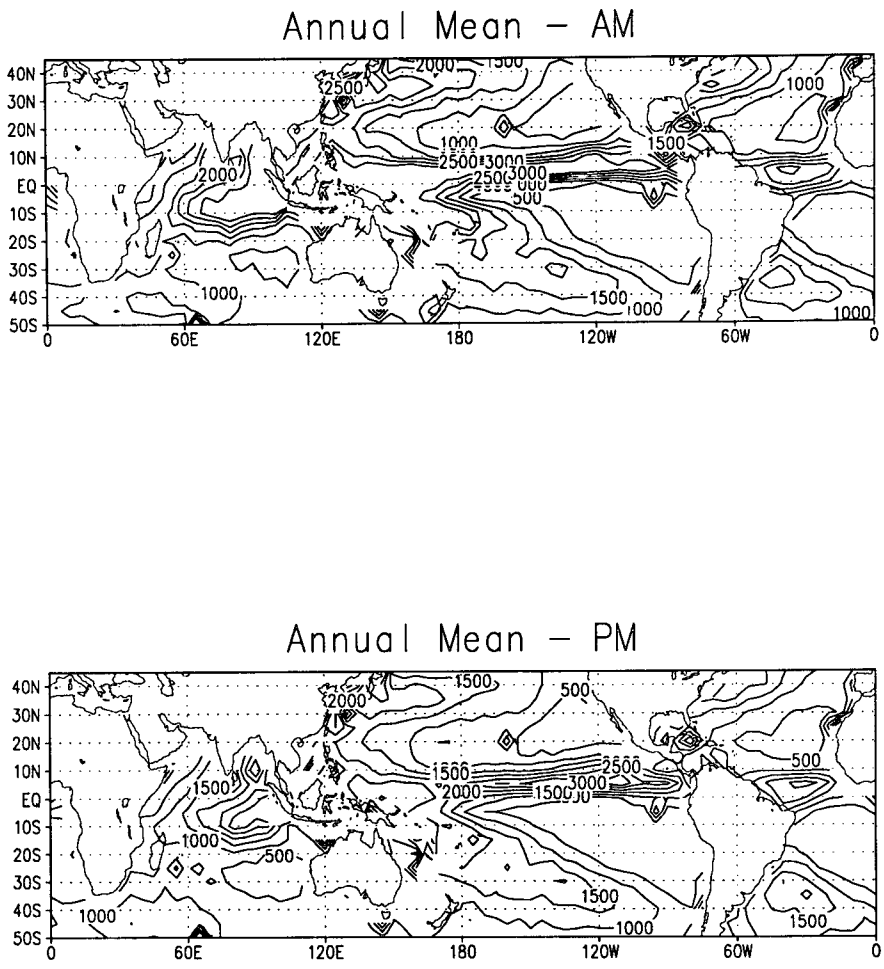

FIG. 1. Annual average rainfall (mm yr^{-1}) derived from SSM/I data for the period July 1987–December 1991 using the Wilheit et al. (1991) algorithm for the morning (upper panel) and evening (lower panel) passes.

spectively. The calibrations of the *F-8* SSM/I sensor were quite stable (Wilheit et al. 1991). In this study we assumed the calibration quality of the data from these three SSM/I sensors are comparable.

The technique for estimating monthly rain rates from SSM/I data was described in detail by Wilheit et al. (1991). In summary, monthly brightness temperature histograms of a combination of SSM/I channels over a 5° × 5° latitude–longitude box are computed. The combined channel (twice the vertically polarized 19.35-GHz minus the 22.235-GHz vertically polarized brightness temperature) was used to minimize the effect of atmospheric water vapor. A brightness temperature–rain rate (T_B–R) relation, based on Wilheit et al.'s (1977) model, converts the brightness temperature histogram to a rain-rate distribution, which is constrained to be lognormally distributed. From the rain-rate distribution, parameters of the rain-rate distributions, such as percent of rainy pixels, means, and variance of rain rate conditional on rain are estimated. Monthly mean rain rates over the 5° × 5° boxes are calculated.

Studies have shown that microwave rainfall estimates tend to underestimate the rain rate due to the beam-filling problem (Chiu et al. 1990; Short and North 1990). The beam-filling error arises due to 1) inhomogeneity within the field of view of the microwave sensor and 2) nonlinearity in the T_B–R relations. Chiu et al. (1990) showed that the beam-filling bias can be expressed as a product of a function of the T_B–R relation and the rain-rate variance. Based on a recent study by Chiu and Chang (1995, unpublished manuscript) the percentage bias for the combination of the 19- and 22-GHz channels is about 35% for convective rainfall. For stratiform rainfall the bias is about 20%. The beam-filling bias is dependent on the rain type,

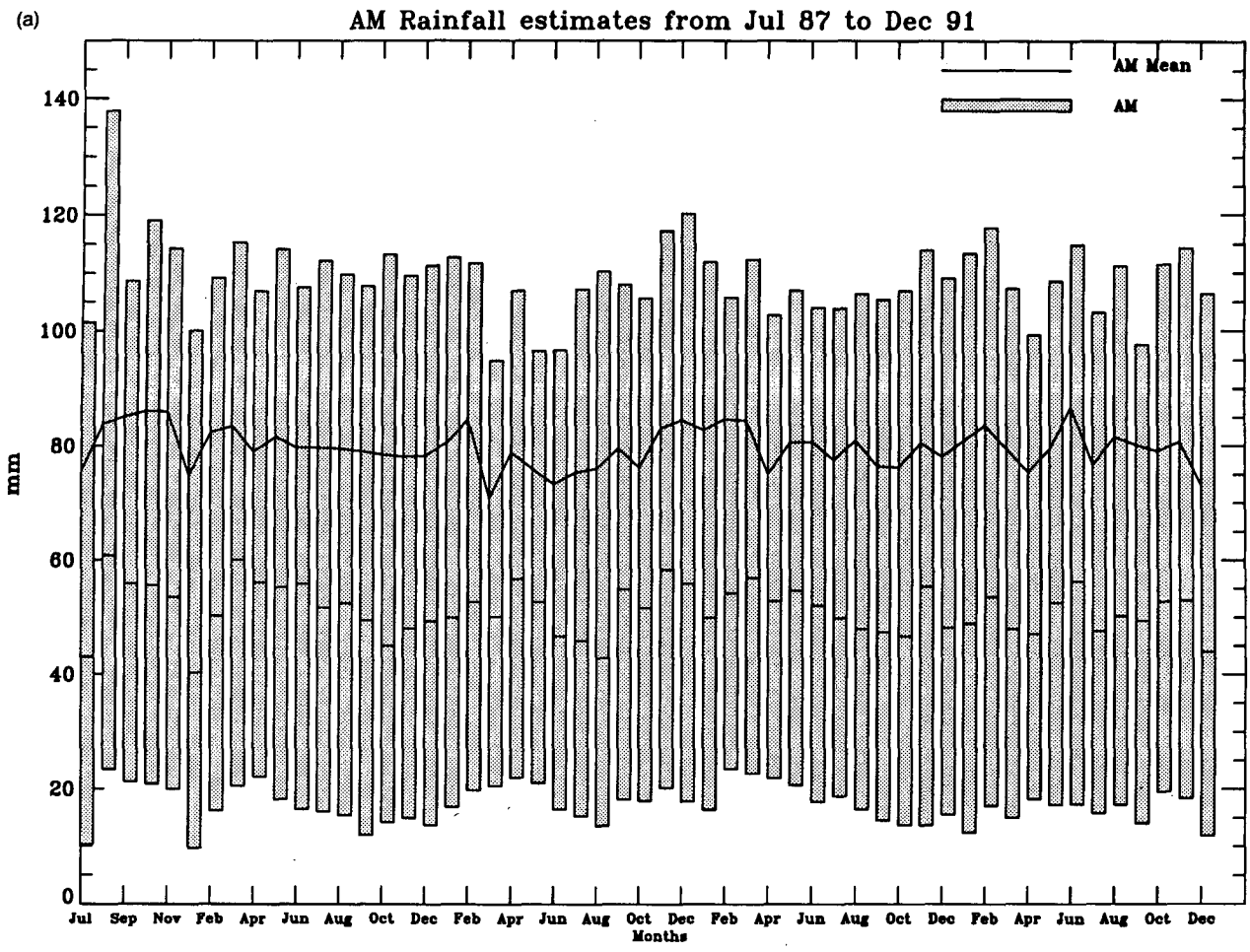

FIG. 2a. Time series of the mean, median, and lower and upper quartiles of the monthly rain rates based on the morning measurements for all grid boxes.

such as convective and stratiform rain and, therefore, can vary diurnally. Given the lack of a differentiation scheme for rain type using microwave measurements, a constant beam-filling bias correction is applied to the estimated monthly rain rates. This would introduce an error of about 20% in the rain-rate measurements.

3. Analysis method

a. Paired t test

We partition the SSM/I data into two groups, namely, the morning $\{X_{Dj}\}$ and evening $\{X_{Nj}\}$ datasets. We wish to test the significance of the difference between the morning and evening data. Let

$$Y_j = X_{Dj} - X_{Nj}, \quad j = 1, 2, \cdots, 53,$$

where $j = 1$ corresponds to July 1987 and $j = 53$ corresponds to December 1991. (December 1987 is missing.)

In general the 53 morning and evening monthly datasets are correlated due to seasonal and other meteorological factors and, hence, cannot be considered independent. To reduce the correlation among the 53 monthly datasets, we perform a paired t test, so that the data can be considered independent (cf. Hines and Montgomery 1990). We also assume the sample distribution to be (approximately) normal, in light of the sample size that is greater than 40.

We want to test the null hypothesis H_0: $\bar{Y} = 0$ versus the alternative hypothesis H_1: $\bar{Y} \neq 0$, where

$$\bar{Y} = E[Y] = E[X_D] - E[X_N] = \bar{X}_D - \bar{X}_N.$$

Let

$$t_0 = \frac{Y}{(n^{1/2}\mathrm{SD})},$$

where Y and SD are the sample mean and standard deviation

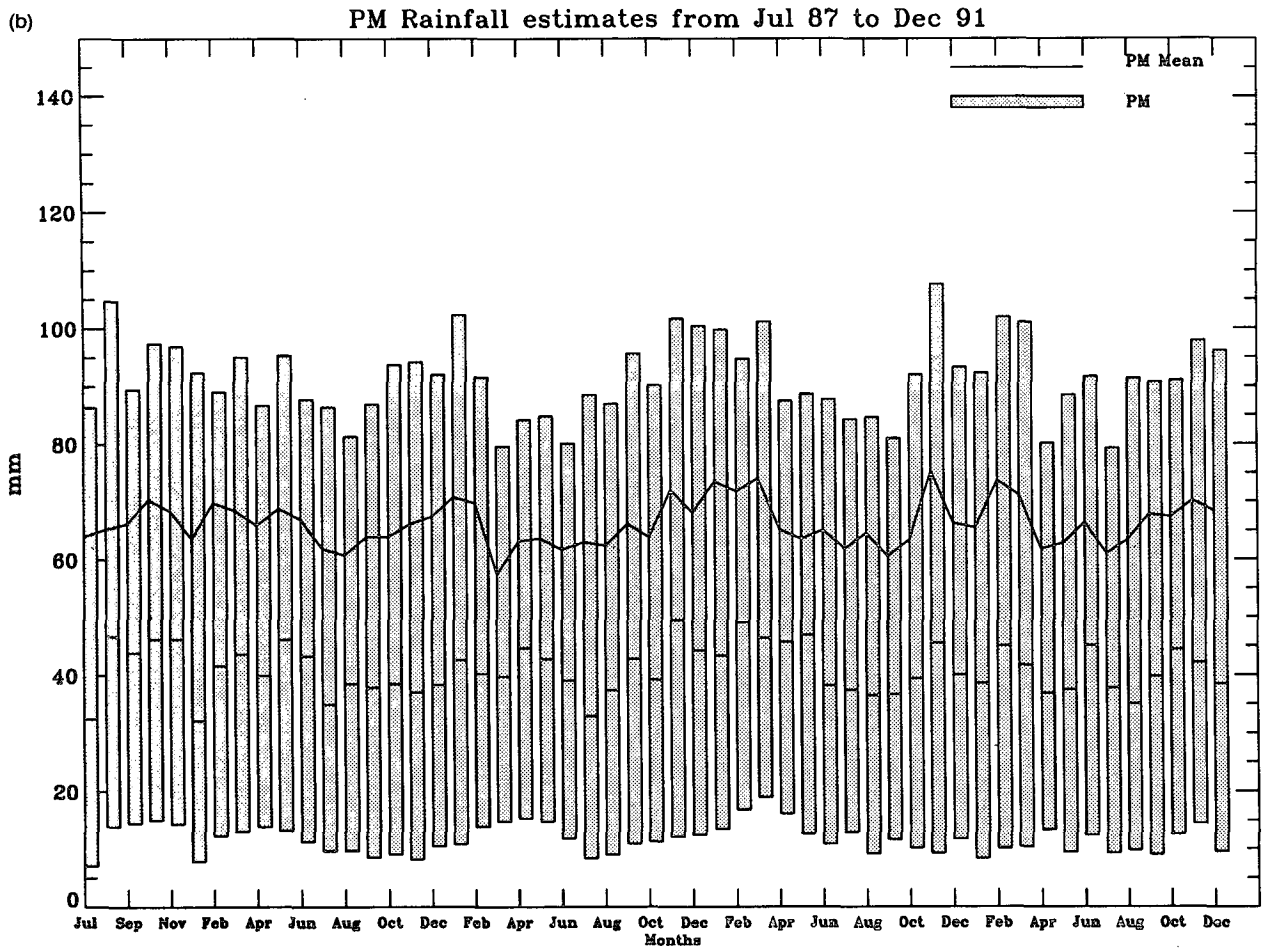

FIG. 2b. Time series of the mean, median, and lower and upper quartiles of the monthly rain rates based on the evening measurements for all grid boxes.

$$Y = \frac{1}{n} \sum Y_i$$

and

$$\mathrm{SD} = \left[\frac{1}{n-1} \left(\sum Y_i^2 - nY^2 \right) \right]^{1/2}.$$

Since t_0 has a t distribution with $n - 1$ degrees of freedom, we shall reject H_0 if $|t_0| > t_{\alpha,n-1}$ and accept H_0 otherwise. For $\alpha = 0.025$, $t_{\alpha,n-1} = 1.96$, for $n > 30$.

b. Estimation of 24-h harmonic

The DMSP satellites were launched into sun-synchronous orbits, with the equator crossing time approximately constant every day. The availability of two SSM/Is (four samples per day) provides an opportunity to examine the diurnal cycle in more detail using Fourier analysis techniques. An estimation scheme for the mean, amplitude and phase of the 24-h harmonic, and the associated error in the estimation is given in appendix A.

4. Results

Figure 1 shows the annual mean rainfall computed from the SSM/I morning and evening data (July 1987–December 1991). Major features such as the ITCZ and the SPCZ are readily evident. The annual rainfall estimates from the morning and evening passes after applying the beam-filling correction of 1.5 are 1444 and 1188 mm yr^{-1}, respectively, over the oceanic region between ±50° latitude. [If a beam-filling correction factor of 1.25 (for stratiform rain) is used, the morning and evening annual rainfalls are 1203 and 990 mm yr^{-1}, respectively.] The ratio of morning to evening rain estimates is about 1.22. This value is consistent with 1.2 reported by Sharma et al. (1991) and 1.27 by Petty and Katsaros (1992). The average of the morning and evening rainfall is 1316 mm yr^{-1} (1097 mm yr^{-1} if a beam-filling correction

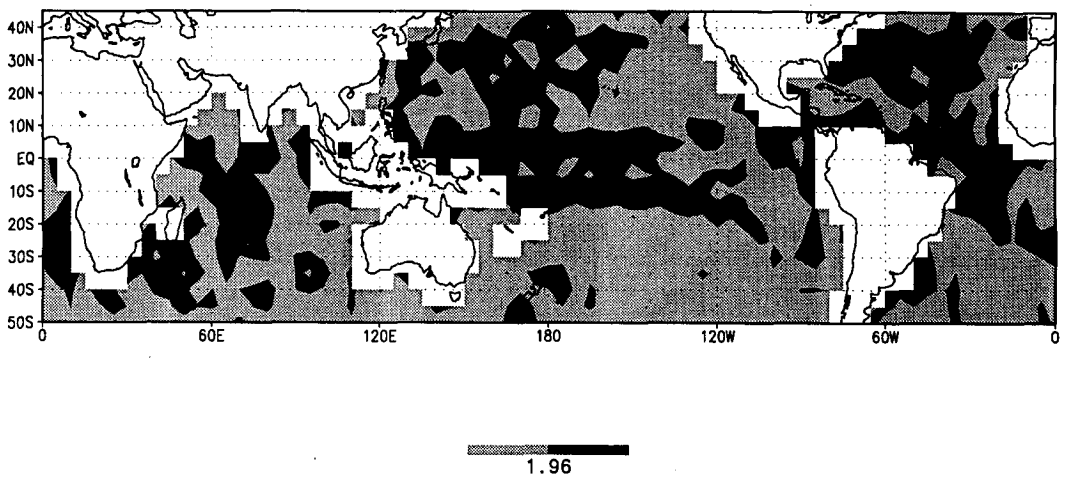

FIG. 3. Distribution of the paired t test values for 53 months of morning and evening data. Areas with $t > 1.96$ are shaded.

factor of 1.25 is used), which can be compared to 1120 mm yr^{-1} based on water budget analysis (Eagleson 1970), 1066 mm yr^{-1} by Baumgartner and Reichel (1975), and 1000 mm yr^{-1} compiled from Jaeger's (1983) and Legates and Willmott's (1990) climatology. The zonally averaged January precipitation derived from published GCM results varies by more than 50% (Simpson 1989). Therefore, the SSM/I rain estimates are consistent with published climatological values.

For all 53 months, the estimated global mean and standard deviation for the morning estimate is larger than for the evening estimate. Because the distribution of the monthly histogram is skewed, it is not sufficient to consider only the mean and standard deviation. Figures 2a and 2b show the means, medians, and lower and upper quartiles (25% and 75%) of the 53 months for both the morning and evening rain rate, respectively. The means are larger than the median, which demonstrates the skewness of the distribution. Like the mean and standard deviation, the median, and lower and upper quartiles from the morning estimates are always greater than the corresponding evening values. The interquartile range for morning estimates is also greater than for evening estimates.

Figure 3 shows the oceanic areas where the value of t_0 is larger than 1.96. These areas constitute about 51% of the oceanic grid boxes. For these grid boxes, there is a significant difference between the daytime and nighttime rainfall. The areas where $|t_0|$ is greater than 1.96 (i.e., where morning-minus-evening difference is significant at the 95% confidence level) are mostly located in the heavy rain regions. This is consistent with results from previous studies: diurnal cycles are most pronounced in regions with strong convective activity. The areas where the $|t_0|$ is less than 1.96 are found mostly in the regions where the diurnal amplitude is known to be small (Hendon and Woodberry 1993).

The derived amplitude for the 24-h harmonic is about 50% of the mean for these two months. The errors in the amplitude and phase estimates were computed by Monte Carlo simulations. By injecting different errors in the morning and evening rain-rate estimates and using different sampling times, errors in the mean, diurnal amplitude, and phase angle are calculated. Figure 4 shows the error in the amplitude estimates as a function of the measurement errors in the morning and evening rain rates and the time separation of the satellite observations. The errors in the estimated amplitude and phase increases with the rain-rate error and the separation in sampling time. The optimal separation is 6 h. With 6-h separation for each of the four samples and a 10% error in the estimated rain rates, the

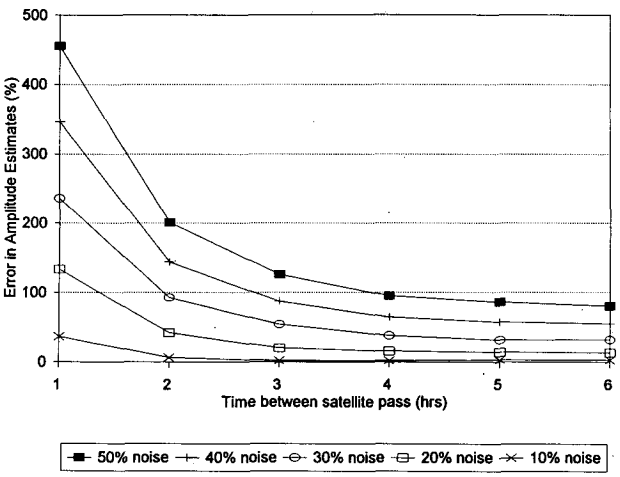

FIG. 4. The errors in the 24-h harmonic amplitude estimates as a function of the measurement error and separation intervals between DMSP sampling times.

diurnal amplitude can be predicted with an accuracy to better than 5%.

The sampling time of these two groups of satellites are not optimum for diurnal study. The separation time between the *F-8* (0600 LT) and *F-10* (0755–0830 LT) overpass is about 2 h and about 3.5 h between the *F-10* and *F-11*. The random error associated with the Wilheit et al. (1991) monthly rain estimates is about 50% (Chang et al. 1993). Hence, from Fig. 4, the error of the amplitude estimate is about 150% for the *F-8* and *F-10* combination and about 90% for the *F-10* and *F-11* combination. The mean residual error associated with the mean estimates are 11.5 and 9.6 mm per month for May 1991 and 1992. An error analysis of the 24-h harmonic was conducted, and the results are summarized in appendix B.

Figure 5 shows the amplitude and phase of the 24-h harmonic for May 1991 and May 1992. The pattern of the 24-h harmonic for May 1991 is less orderly than that of May 1992. We have applied the same analysis to the May 1993 data (results not shown). The 24-h harmonic of the May 1993 data showed a similar pattern to that of May 1992. The difference in the pattern is consistent with error estimates discussed above: the errors are higher in May 1991 (150%) than in May 1992 (90%). With a 50% random error in the rainfall estimates, the standard error of the phase angle estimate is about 2 h. Due to this large uncertainty in phase

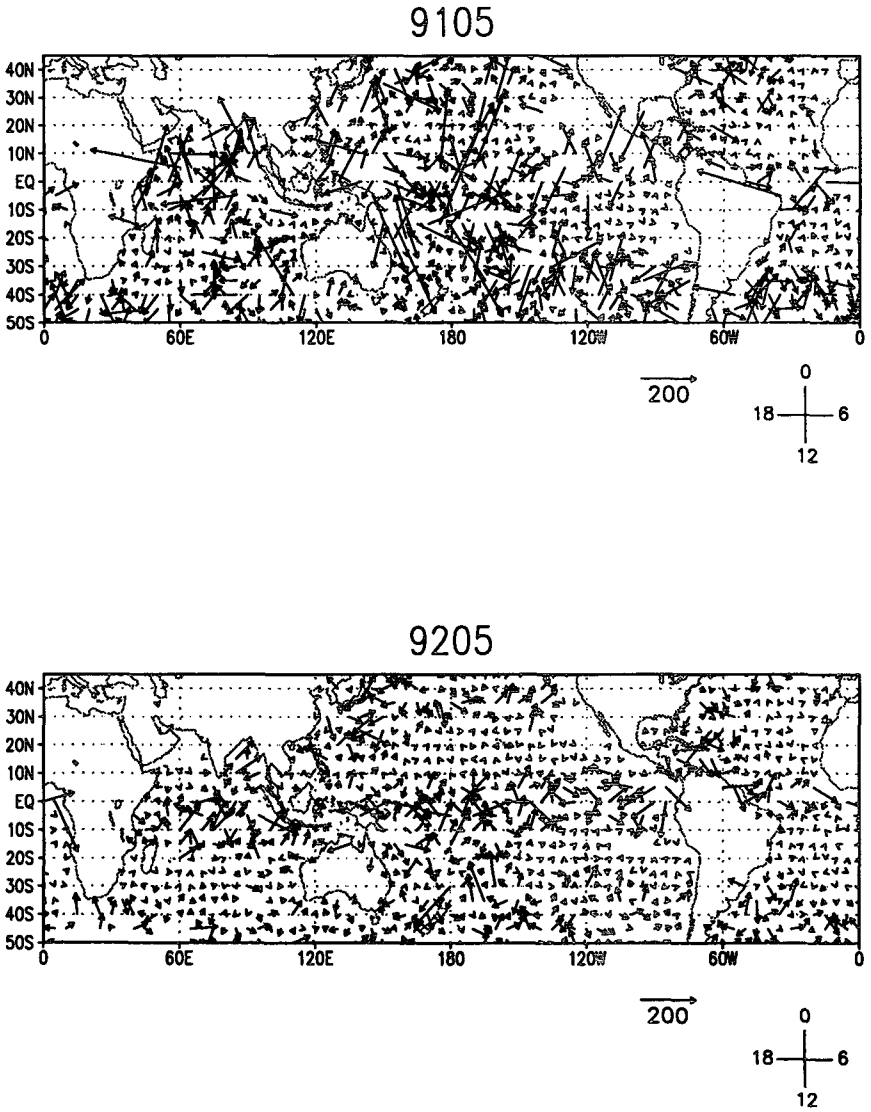

FIG. 5. Amplitude and phase of the 24-h harmonic for May 1991 (upper) and May 1992 (lower panel). The length of the vector represents the amplitude, and the angle with respect to north represents the phase.

TABLE 1. Oceanic rainfall distribution for 6-h time periods.

	May 1991			May 1992		
	Atlantic	Indian	Pacific	Atlantic	Indian	Pacific
0000–0600 LT	39%	38%	37%	34%	37%	36%
0600–1200 LT	24%	21%	26%	30%	28%	27%
1200–1800 LT	14%	16%	16%	18%	17%	17%
1800–2400 LT	23%	25%	21%	18%	18%	20%

determination, phase angles were binned in 6-h periods for comparison. The most frequent rain period is the early morning (0000–0600 LT); it accounted for 37% and 36% for all the grid boxes for May 1991 and 1992, respectively. The least frequent period is early afternoon (1200–1800 LT) for these two months (16% and 17% respectively). The distributions of time of maximum rainfall over the Atlantic, Pacific, and Indian Oceans are very similar and are tabulated in Table 1. These results are consistent with the results reported by Gray and Jacobson (1977) and Hendon and Woodberry (1993). If one divides day and night following Kraus's (1963) convention, then 64% of the rain maximum occurs during the night (2100–0900 LT) and 36% during the day (0900–2100 LT) for May 1991. The corresponding distributions are 68% (2100–0900 LT) and 32% (0900–2100 LT) for May 1992.

5. Discussion

Four and a half years of monthly oceanic rain rates derived from SSM/I data are used to examine the diurnal cycle in oceanic precipitation. The averaged monthly morning estimates are larger than the evening estimates for each of the 53 months by about 22%. Based on a paired t test, the differences between morning and evening rain estimates are significant at the 95% level for 51% of the 5° latitude by 5° longitude grid boxes. The areas in which evening rain are larger than morning rain are mostly located in regions where the rain total is small, such as the southern Pacific and Atlantic Ocean dry zones.

In lack of a differentiation scheme for the rain type, a constant beam-filling correction factor has been applied to both morning and evening estimates. The analysis of Mapes and Houze (1993) showed that deep convection is strongest in the early morning and decreases as the day progresses. The afternoon maximum of moderately cold clouds is indicative of shallower convection. Hence, we can expect that the morning precipitation is of a more convective nature than that in the afternoon. Hence, a higher beam-filling correction factor would apply to the morning rain estimates, enhancing the morning–evening difference.

Harmonic analysis has been developed to estimate the mean rain rate and amplitude and phase of the 24-h harmonics. They showed a nocturnal and early morning maximum in most oceanic areas where the total precipitation is high. Our results are therefore consistent with the theories of day–night radiation difference in explaining the oceanic rainfall diurnal cycle proposed by Kraus. However, based on the results of Monte Carlo simulations, optimal amplitude and phase estimates require accurate rainfall estimates and a satellite observing time separation of 6 h. The times for overpasses between *F-8* and *F-10* and between *F-10* and *F-11* are 2 and 3.5 h, respectively, and hence are not optimal. The harmonic analysis results presented herein must therefore be taken with caution.

Acknowledgments. The authors thank H. Powell, C. Tsai, V. Kuan, and J. Chien of SAIC/General Sciences Corporation (GSC) for programming and graphics assistance. This work was partially supported by the Office of Mission to Planet Earth, the National Aeronautics and Space Administration, and the Global Climate Change Program Office, National Oceanic and Atmospheric Administration.

APPENDIX A

Optimal Estimation of the Mean, 24-h Harmonic Amplitude and Phase of the Diurnal Cycle, and Error

Let the diurnal variation of rainfall be represented as follows:

$$R(t) = A + B\cos(\omega t + \delta + \theta) + e, \quad \text{(A1)}$$

where A is the mean; B and δ are the amplitude and phase of the 24-h harmonic of the diurnal cycle; $\omega = 2\pi/P$, where P is the period (24 h); e is the residual error; and θ is a constant phase bias. We can expand the double angle and write

$$R(t) = A + a\cos\omega t + b\sin\omega t + e, \quad \text{(A2)}$$

where $a = B\cos(\delta + \theta)$ and $b = -B\sin(\delta + \theta)$. Hence the amplitude and phase can be written as

$$B = (a^2 + b^2)^{1/2} \quad \text{(A3)}$$

and

$$\delta = \tan^{-1}\left(-\frac{b\cos\theta - a\sin\theta}{a\cos\theta + b\sin\theta}\right). \quad \text{(A4)}$$

Note that the net effect of the addition of a constant phase bias is to add weights to the a's and b's in the estimation. The choice of the phase bias is determined by the relative magnitude of a and b. Such a bias would minimize spurious errors in the phase estimates when $|a|$ or $|b|$ are small.

The DMSP *F-8* (*F-10*) satellite makes observations at roughly 0610 (0755) local time for the ascending node and 12 h later for the descending node. Recognizing that the observations are 12 h (half of the period)

apart and using the identities $\cos(x + \pi) = -\cos(x)$ and $\sin(x + \pi) = -\sin(x)$, we can write

$$R_1 = R(t_1) = A + a\cos\omega t_1 + b\sin\omega t_1 + e_1 \quad \text{(A5)}$$

$$R_2 = R(t_2) = A + a\cos\omega t_2 + b\sin\omega t_2 + e_2 \quad \text{(A6)}$$

$$R_3 = R(t_3) = R(t_1 + 12)$$
$$= A - a\cos\omega t_1 - b\sin\omega t_1 + e_3 \quad \text{(A7)}$$

$$R_4 = R(t_4) = R(t_2 + 12)$$
$$= A - a\cos\omega t_2 - b\sin\omega t_2 + e_4, \quad \text{(A8)}$$

where A is the mean, a and b are the coefficients of the cosine and sine term, and the e's are the residual errors of the estimation. The above equations can be written in matrix notation as

$$\mathbf{R} = \mathbf{MC} + \mathbf{e}, \quad \text{(A9)}$$

where $\mathbf{R} = (R_1, R_2, R_3, R_4)^T$, $\mathbf{e} = (e_1, e_2, e_3, e_4)^T$ are 4×1 vectors, $\mathbf{C} = (A, a, b)^T$ is a 3×1 vector, and $\mathbf{M}$ is a 4×3 matrix of the form

$$\mathbf{M} = \begin{bmatrix} 1 & \cos\omega t_1 & \sin\omega t_1 \\ 1 & \cos\omega t_2 & \sin\omega t_2 \\ 1 & -\cos\omega t_1 & -\sin\omega t_1 \\ 1 & -\cos\omega t_2 & -\sin\omega t_2 \end{bmatrix}. \quad \text{(A10)}$$

The error can be written as

$$\mathbf{e}^T\mathbf{e} = \mathbf{R}^T\mathbf{R} - \mathbf{C}^T\mathbf{M}^T\mathbf{R} - \mathbf{R}^T\mathbf{MC} + \mathbf{C}^T\mathbf{M}^T\mathbf{MC}. \quad \text{(A11)}$$

The solution $\mathbf{C}_0$ that minimizes the error $\mathbf{e}^T\mathbf{e}$ is

$$\mathbf{C}_0 = (\mathbf{M}^T\mathbf{M})^{-1}\mathbf{M}^T\mathbf{R}. \quad \text{(A12)}$$

Hence, given the four measurements, $\mathbf{R}$, the mean, amplitude, phase, and the error term can be computed.

APPENDIX B

Error Analysis

The optimal estimates can be written as

$$A_0 = \frac{(R_1 + R_2 + R_3 + R_4)}{4} \quad \text{(B1)}$$

$$a_0 = \frac{C_1(R_1 - R_3) + C_2(R_2 - R_4)}{2(C_1^2 + C_2^2)} \quad \text{(B2)}$$

$$b_0 = \frac{S_1(R_1 - R_3) + S_2(R_2 - R_4)}{2(S_1^2 + S_2^2)}, \quad \text{(B3)}$$

where $S_1 = \sin\omega t_1$, $S_2 = \sin\omega t_2$, $C_1 = \cos\omega t_1$, and $C_2 = \cos\omega t_2$.

The estimated mean A_0 is simply the arithmetic average of the observations, whereas the cosine and sine terms a_0 and b_0 involve only the difference between the morning and evening measurements. Assuming there are measurement–retrieval errors in the $\mathbf{R}$, that is,

$$\mathbf{R} = \mathbf{R} + \delta\mathbf{R}, \quad \text{(B4)}$$

it can be shown that the errors made in $\mathbf{C}_0$ or $\delta\mathbf{C}_0$ are linearly related to $\delta\mathbf{R}$:

$$\delta\mathbf{C}_0 = (\mathbf{M}^T\mathbf{M})^{-1}\mathbf{M}^T\delta\mathbf{R}. \quad \text{(B5)}$$

The estimate of the mean A_0 is insensitive to random errors in the measurement but is proportional to the bias in the measurements. Conversely, the errors in estimating the diurnal amplitude are dependent only on the difference between the morning and evening measurements of same satellite; thus, the amplitude estimate is not sensitive to biases in measurements using the same satellite. The model breaks down in the case when the observation times are close to one another; that is, $t_1 = t_2$.

REFERENCES

Albright, M. D., E. E. Recker, R. J. Reed, and R. Dang, 1985: The diurnal variation of deep convection and inferred precipitation in the central tropical Pacific during January–February 1979. *Mon. Wea. Rev.*, **113**, 1663–1680.

Baumgartner, A., and E. Reichel, 1975: *World Water Balance.* Oldenbourg, 179 pp.

Chang, A. T. C., L. S. Chiu, and T. T. Wilheit, 1993: Random errors of oceanic monthly rainfall derived from SSM/I using probability distribution functions. *Mon. Wea. Rev.*, **121**, 2153–2156.

Chiu, L. S., G. R. North, D. A. Short, and A. McConnell, 1990: Rain estimation from satellite: Effect of finite field of view. *J. Geophys. Res.*, **95**, 2177–2185.

——, A. T. C. Chang, and J. Janowiak, 1993: Comparison of monthly rain rate derived from GPI and SSM/I using probability distribution functions. *J. Appl. Meteor.*, **32**, 323–334.

Eagleson, P. S., 1970: *Dynamic Hydrology.* McGraw-Hill, 462 pp.

Gray, W. M., and R. W. Jacobson Jr., 1977: Diurnal variation of deep cumulus convection. *Mon. Wea. Rev.*, **105**, 1171–1188.

Gruber, A., and T. S. Chen, 1988: Diurnal variation of outgoing longwave radiation. *J. Climatol.*, **8**, 1–16.

Hartmann, D. L., and E. E. Recker, 1986: Diurnal variation of outgoing longwave radiation in the tropics. *J. Climate Appl. Meteor.*, **25**, 800–812.

Hendon, H. H., and K. Woodberry, 1993: The diurnal cycle of tropical convection. *J. Geophys. Res.*, **98**, 16 623–16 637.

Hines, W., and D. Montgomery, 1990: *Probability and Statistics in Engineering and Management Science.* John Wiley & Sons, 634 pp.

Jaeger, L., 1983: Monthly and areal patterns of mean global precipitation. *Variation in the Global Water Budget,* A. Street-Perrott et al., Eds., D. Reidel Publishing, 129–140.

Janowiak, J. E., and P. A. Arkin, 1991: Rainfall variations in the tropics during 1986–1989, as estimated from observations of cloud-top temperature. *J. Geophys. Res.*, **96**(Suppl.), 3359–3373.

Kidder, S. Q., and T. H. Vonder Haar, 1977: Seasonal oceanic precipitation frequencies from Nimbus-5 microwave data. *J. Geophys. Res.*, **82**, 2083–2086.

Kraus, E. B., 1963: The diurnal precipitation change over the sea. *J. Atmos. Sci.*, **20**, 551–556.

Legates, R. D., and C. J. Willmott, 1990: Mean seasonal and spatial variability in gauge-corrected precipitation. *Int. J. Climate,* **10**, 111–127.

Mapes, B. E., and R. A. Houze Jr., 1993: Cloud clusters and superclusters over the oceanic warm pool. *Mon. Wea. Rev.*, **121**, 1398–1415.

McGarry, M. A., and R. J. Reed, 1978: Diurnal variation in convective activity and precipitation during phases II and III of GATE. *Mon. Wea. Rev.*, **106**, 101–113.

Meisner, B., and P. Arkin, 1987: The relationship between large-scale convective rainfall and cold loud over the Western Hemisphere during 1982–84. *Mon. Wea. Rev.*, **115,** 51–74.

Petty, G. W., and K. K. Katsaros, 1992: Morning-evening differences in global and regional oceanic precipitation as observed by the SSM/I. *Proc. of the Satellite Meteorology Conf.,* Atlanta, GA, Amer. Meteor. Soc., 282–285.

Riehl, H., and A. M. Miller, 1978: Differences between morning and evening temperatures of cloud tops over tropical continents and oceans. *Quart. J. Roy. Meteor. Soc.*, **104,** 757–764.

Sharma, A., A. Chang, and T. Wilheit, 1991: Estimation of the diurnal cycle of oceanic precipitation from SSM/I data. *Mon. Wea. Rev.*, **119,** 2168–2175.

Shin, K.-S., G. R. North, Y.-S. Ahn, and P. A. Arkin, 1991: Time scales and variability of area-averaged tropical oceanic rainfall. *Mon. Wea. Rev.*, **118,** 1507–1516.

Short, D. A., and J. M. Wallace, 1980: Satellite-inferred morning-to-evening cloudiness changes. *Mon. Wea. Rev.*, **108,** 1160–1169.

——, and G. R. North, 1990: The beamfilling error in ESMR-5 observations of GATE rainfall. *J. Geophys. Res.*, **95,** 2187–2194.

Simpson, J., 1989: On climate variability and tropical rain: necessity for space measurement. *Earth Observations and Global Change Decision Making,* I. Ginsberg and J. Angelo, Eds., Krieger, 293–298.

Wilheit, T. T., A. T. C. Chang, M. S. V. Rao, E. B. Rodgers, and J. S. Theon, 1977: A satellite technique for quantitatively mapping rainfall rates over the oceans. *J. Appl. Meteor.*, **16,** 551–560.

——, ——, and L. S. Chiu, 1991: Retrieval of monthly rainfall indices from microwave radiometric measurements using probability distribution functions. *J. Atmos. Oceanic Technol.*, **8,** 118–136.